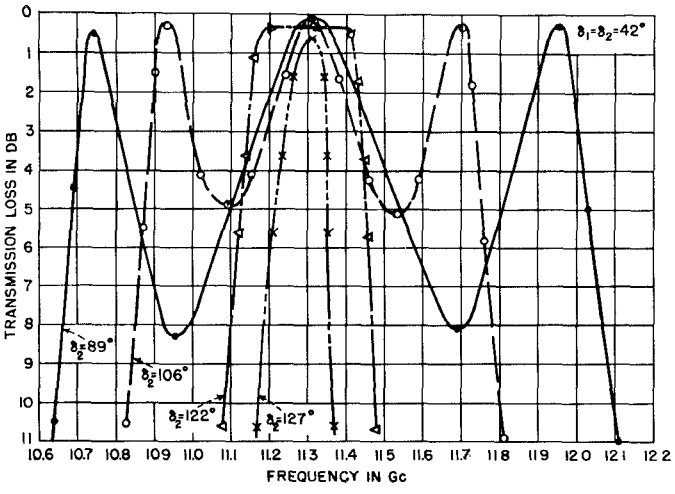

Fig. 8—Transmission characteristics of the filter shown in Fig 5.

advantages for general use of the symmetric, odd cavity configuration with connecting sections aligned are obvious.

Our procedure for obtaining a given characteristic from a direct-coupled cascade is as follows. First, the desired degree of discrimination against frequencies not in the passband, or other pertinent considerations, are used to select the number of cavities desired. An ordinary circular iris cavity, with centered holes whose diameter is the same as the height of the rectangular waveguide, is designed to be resonant at the desired frequency of operation. The iris spacing so obtained is then maintained for all the cavities of the multiple-cavity filter. A cylindrical holder is provided to contain the cavities and allow rotation (see Fig. 5) and, when assembled, the swept transmission and reflection characteristics are simultaneously monitored on a dual-beam oscilloscope. Frequency markers and attenuation calibrations can then be utilized to synthesize the desired filter response.

Conclusions

A theoretical study of the properties of constant-phase two-ports was presented which leads to a simple synthesis technique for a broad class of microwave filters. Constant-phase two-ports consisting of modified step-twist junctions were employed in direct coupled filter configurations whose behavior was predicted from the theory. These filters were shown to have the unique property of adjustable band-pass characteristic and fixed center frequency.

Acknowledgment

The author is pleased to acknowledge the assistance of S. F. Jankowski who made all the measurements and did the mechanical design work on the filter structures. The author is further indebted to E. A. Marcatili for several helpful suggestions with the manuscript.

Some Aspects of the Design of Wide-Band Up-Converters and Nondegenerate Parametric Amplifiers*

W. J. GETSINGER†, MEMBER, IEEE, AND G. L. MATTHAEI‡, MEMBER, IEEE

Summary—Proper design of the diode-resonating circuit is seen to be extremely important if large bandwidth is desired in a varactor-diode parametric amplifier. Cases where there is one resonance of the diode-resonating circuit at a frequency between the frequencies of the signal-input and the sideband resonances are examined in some detail. It is shown that the frequency of this intermediate resonance can greatly influence the bandwidth capabilities of an amplifier design, and the optimum frequency for such a resonance is given for upper-sideband up-converters. The optimum frequency of such a resonance is greatly different if the diode is resonated in series than it is if the diode is resonated in shunt. It is believed that the same results would also apply for lower-sideband up-converters and nondegenerate parametric amplifiers. Some upper-sideband up-converter designs were worked out and their computed responses are given including the effects of all of the parasitic elements of the diode. Bandwidths of the order of an octave are obtained. A systematic design procedure is given for wide-band nondegenerate parametric amplifiers which use the diode parasitic resistance as the idler termination. Some designs of this type were also worked out and their computed responses (including effects of all diode parasitic parameters) are presented. Bandwidths as large as 33 per cent are obtained depending on the peak gain and operating frequency range.

I. Introduction

IT HAS BEEN shown previously[1] that single-diode parametric amplifiers and up-converters using multiple-resonator filters as coupling networks can be made to have considerably larger bandwidths than corresponding amplifiers having single-resonator coupling circuits. The present paper investigates the practical design of the circuitry used to resonate the diode at two

* Received July 9, 1963. This research was supported by American Electronics Laboratories, Inc., Colmar, Penn.

† Lincoln Laboratories, Lexington, Mass. Formerly with Stanford Research Institute.

‡ Stanford Research Institute, Menlo Park, Calif.

[1] G. L. Matthaei, "A study of the optimum design of wide-band parametric amplifiers and up-converters," IRE Trans. on Microwave Theory and Techniques, vol. MTT-9, pp. 23–38; January, 1961.

frequencies, and shows how this circuitry affects the bandwidth of the amplifier for both series and shunt connections of the diode. The results of this investigation are then applied to the design of shunt-connected up-converters and parametric amplifiers, using the filter techniques described by Matthaei.[1] Then, gain curves are computed as functions of frequency, taking into account the diode resistance, inductance, and cartridge capacitance.

The point of view of this paper follows that of Matthaei[1] very closely, and familiarity with the concepts in that paper is assumed of the reader.

II. The Diode Circuitry

A critical examination was made of the bandwidth determining factors in upper- and lower-sideband up-converters. This examination showed that for a diode with no series inductance and resistance, and with no capacitance shunting the cartridge, it was possible to obtain the same bandwidth for either the series or shunt connection of the diode, provided that the diode circuitry is properly designed for the given type of connection. By "diode circuitry" is meant the reactive structure which brings the diode to resonance at the input-signal and output-signal frequencies.

Briefly, the most critical step in designing an up-converter or parametric amplifier for wide bandwidth is in the selection of the circuitry to resonate the diode. In order to obtain maximum bandwidth, it is necessary to minimize the number of resonances of the diode circuit, and to keep the slope of the diode reactance or susceptance characteristic in the vicinity of the resonances at the signal and the sideband frequencies as low as possible.[1] In this regard, Bossard and Pettai[2] have made use of the natural series resonance of the diode at the signal frequency, and the natural parallel resonance of the diode at the sideband (or idler) frequency. This approach should give the best possible bandwidth capabilities from the diode circuit, but it has the disadvantage of requiring the diode to have very specific parameters. In the approach of this paper, the diode parasitic elements are supplemented by resonating elements external to the diode so that adjustments can be made to accommodate a range of diode parameters Also, instead of the diode being series resonated at the signal frequency and parallel resonant at the sideband frequency, herein the diode circuit will have the same type of resonance at both the signal and sideband frequencies.

A *shunt*-connected diode and its resonating circuitry, considered as essentially lossless, must have a *zero of susceptance* at both the input-signal and the output-signal midband frequencies. Physical realizability requires that there be at least one *pole of susceptance* between two zeros. (Note, if there is more than one pole in between, Foster's reactance theorem requires that there also be additional zeros in between.) Analogously, for the *series*-connected case the diode plus its resonating circuit must give a *zero of reactance* at both the input and output frequencies, and at least one *pole of reactance* in between. Thus, the susceptance or the reactance function of the diode and its circuitry can be represented by nothing simpler than Kuh and Fukada's mapping function[3]

$$K\frac{(s^2+\omega_0^2)(s^2+\omega_0'^2)}{s(s^2+\omega_\infty^2)},$$

where

K is a constant,
$s=\sigma+j\omega$ represents complex frequency,
ω_0 is the signal-input center frequency,
ω_0' is the signal-output center frequency, and
ω_∞ is the frequency of the pole lying between ω_0 and ω_0'.

Kuh and Fukada specified ω_∞ to be specifically $\sqrt{(\omega_0^2+\omega_0'^2)/2}$; however, in this research the effect of using other values of ω_∞ was also studied.

It can be shown that having only one pole between frequencies ω_0 and ω_0' will lead to the greatest bandwidth. Further, our studies have shown that the obtainable bandwidth is quite sensitive to the frequency ω_∞ at which the pole occurs, and that the optimum value for ω_∞ is radically different for the shunt-connected diode than for the series-connected diode. For example, if $\omega_0/2\pi=1$ Gc and $\omega_0'/2\pi=10$ Gc, neglecting diode package capacitance and series inductance, the optimum value of $\omega_\infty/2\pi=7.1$ Gc for the shunt-connected case, while the optimum value is $\omega_\infty/2\pi=1.41$ Gc for the series-connected case. Under these conditions the same bandwidth is possible for either connection.

The material in Fig. 1 is based on the use of diode-resonator reactance or susceptance functions having the form of the mapping function used by Kuh and Fukada.[3] The figure treats the cases of upper-sideband up-converters having a series connection for the diode (oversimplified since it assumes no package capacitance), a shunt connection for the diode (oversimplified since it assumes no inductance in series with the diode), and a shunt connection for the diode with both series inductance and diode package capacitance present. The first two circuits are relatively simple to analyze and allow exact comparison of series and shunt connection. The last circuit is important because it includes all of the reactive parameters needed to accurately represent the

[2] B. B. Bossard and R. Pettai, "Broad-band parametric amplifiers by simple experimental techniques," Proc. IRE (*Correspondence*), vol. 50, pp. 328–329; March, 1962.

[3] E. S. Kuh and M. Fukada, "Optimum synthesis of wide-band parametric amplifiers and converters," IRE Trans. on Circuit Theory, vol. CT-8, pp. 410–415; December, 1961.

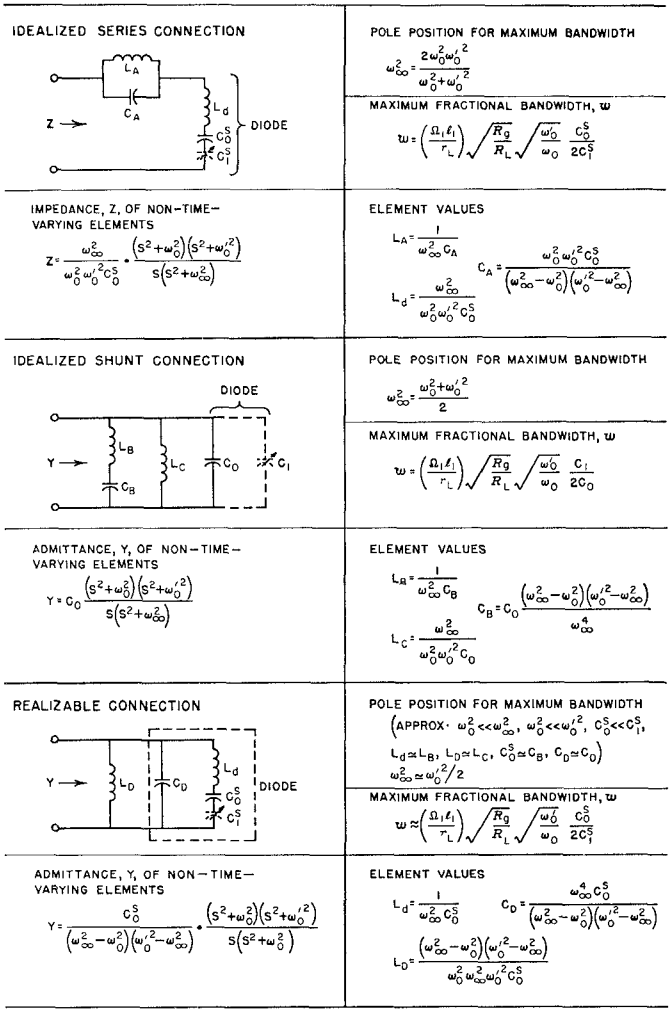

Fig. 1—Various diode connections and equations for use in the design of upper-sideband up-converters.

diode. The pole location ω_∞ for maximum bandwidth and the maximum fractional bandwidth w are exact for the first two cases, and approximate for the last. Note that the value of ω_∞ used by Kuh and Fukada[3] in their analysis of the idealized shunt-resonance case was found to be the optimum value of ω_∞ for that case. However, note that the equation for the optimum ω_∞ for the series-resonated case is quite different. The equations for fractional bandwidth w were derived by the methods of Matthaei,[1] and the parameters shown are as defined and discussed in that reference. It should be noted that

$$C_0^s/C_1^s = C_1/C_0 = a,$$

where the parameters with a superscript s are for the representation of the diode as a fixed and time-varying capacitance in series, while the parameters without superscripts are for the usual representation with the fixed and time-varying components in parallel.

The equality above, substituted in the fractional bandwidth equations of Fig. 1, shows that the three forms all are capable of the same maximum bandwidth (or nearly the same bandwidth) when the pole location ω_∞ is properly chosen. Of course, the last connection shown, a shunt connection, is preferable to the other two, because it allows both the series inductance and shunt capacitance associated with an actual diode cartridge to be incorporated into the diode circuitry.

As an example, assume idealized lumped elements as in the table and determine the maximum fractional bandwidth of an up-converter using a diode for which $C_1/C_0 = 0.3$. The low-pass prototype filter to be used is that of Fig. 21(b) of Matthaei[1] (or its dual). This results in a design with three input resonators and three upper-sideband output resonators to give over-all performance with Chebychev ripples like those of a six-resonator filter. In Section XI of Matthaei,[1] the prototype element values of interest for calculating the bandwidth are given as

$$l_1 = 2.604,$$
$$r_L = 1.000,$$
$$\mathcal{R}_g = 1.000,$$
$$\mathcal{R}_L = 1.984,$$
$$\Omega_1 = 1.000.$$

Substitution of the above values into one of the fractional bandwidth equations of Fig. 1 gives

$$w = 0.278\sqrt{\frac{\omega_0'}{\omega_0}}.$$

For $\omega_0'/\omega_0 = 10$, a reasonable value, we find that $w = 0.88$ to slide rule accuracy.

The analysis discussed so far assumes idealized lumped-element circuitry. Although such circuitry is usually not realizable in an exact way at microwave frequencies, this lumped-circuit analysis represents an important guide for use in designing practical microwave circuitry. For physically realizable circuitry at microwave frequencies, the shunt inductance L_D in the "Realizable Connection" of Fig. 1 is replaced by a shorted transmission line. Fig. 2(a) is a picture showing how this might be accomplished in practice. The diode is attached to a shorting block between parallel plates, and the shorted line is a length of wire stretching between the diode and another shorting block. Fig. 2(b) gives the equivalent circuit of the structure. The terminal of interest is at the junction of the diode and the shorted stub. When the diode is being pumped the impedance measured at this terminal should be purely real at both the midband signal frequency ω_0, and the midband frequency of the sideband to be used ω_0'. A more useful equivalent circuit is given in Fig. 2(c), where the circuitry to the left of the box labelled $X_{12}X_{21}$ applies only to the signal frequency ω, and the circuitry to the right applies only to ω'. The static

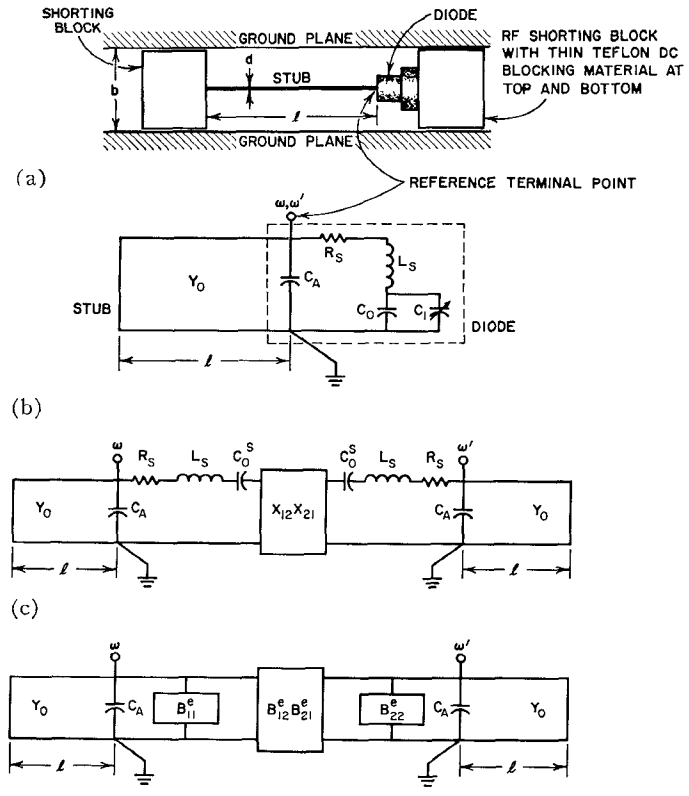

Fig. 2—Physical construction and equivalent circuit for diode circuitry.

capacitance C_0 and the time-varying capacitance C_1 of Fig. 2(b) have been replaced by an equivalent series form involving a series static capacitance C_0^s and the box labelled $X_{12}X_{21}$, which accounts for coupling between the two frequencies. [See (3), (5)–(8) of Matthaei.[1]] The circuit of Fig. 2(c) will be used subsequently, but in order to provide a representation on which conditions of resonance can be imposed at ω_0 and ω_0' simultaneously, it is desirable to further transform the series networks between terminals ω and ω' of Fig. 2(c) into a purely shunt circuit as shown in Fig. 2(d). (R_s has been neglected for this step.) This yields[4]

$$\left.\begin{aligned} B_{11}^e &= \frac{-\gamma'\omega C_0^s}{\gamma\gamma' - a^2} \\ B_{22}^e &= \frac{-\gamma\omega' C_0^s}{\gamma\gamma' - a^2} \\ B_{12}^e &= \frac{a\omega C_0^s}{\gamma\gamma' - a^2} \\ B_{21}^e &= \frac{a\omega' C_0^s}{\gamma\gamma' - a^2} \end{aligned}\right\} \quad (1)$$

[4] G. L. Matthaei, "Design Criteria for Microwave Filters and Coupling Structures," Stanford Research Inst., Menlo Park, Calif., Tech. Rept. No. 11, SRI Project No. 2326, Contract No. DA 36-039 SC-74862; ch. IV, pp. 41–43; September, 1960.

where

$$\gamma = \left(\frac{\omega}{\omega_\infty}\right)^2 - 1$$

$$\gamma' = \left(\frac{\omega'}{\omega_\infty}\right)^2 - 1$$

$$\omega_\infty = \frac{1}{\sqrt{L_d C_0^s}}$$

$$a = C_1/C_0 \quad (2)$$

and

$$\omega' = \omega + \omega_p,$$

where ω_p is the pump frequency.

The parallel combination of the stub and the diode cartridge capacitance must resonate with B_{11}^e at the misband signal frequency ω_0 and with B_{22}^e at the midband upper-sideband frequency ω_0'. This leads to the following formulas for determining parameter values in terms of the diode element values and the length l and diameter d of the stub.

$$\left.\begin{aligned} Y_0 &= \left[\frac{2\pi f_0 C_0^s}{(a^2 - \gamma_0\gamma_0')}\right] \frac{\left[\left(\frac{f_0'}{f_\infty}\right)^2 - \left(\frac{f_0}{f_\infty}\right)^2\right]}{\left[\cot\frac{2\pi f_0 l}{c} - \frac{f_0}{f_0'}\cot\frac{2\pi f_0' l}{c}\right]} \\ d/b &= \frac{4}{\pi}\exp\left[-\frac{2\pi\sqrt{\epsilon_r}}{\eta Y_0}\right] \\ C_A &= \frac{\gamma_0 C_0^s}{(\gamma_0\gamma_0' - a^2)} + \frac{y_0}{2\pi f_0'}\cot\frac{2\pi f_0' l}{c} \end{aligned}\right\} \quad (3)$$

where

$\eta = 376.7$ ohms,

c = velocity of propagation,

ϵ_r = relative dielectric constant

and the subscript 0 indicates values at band-center frequencies.

Fig. 3 shows the values that C_A and d/b are required to take for various values of the diode resonant frequency ω_∞ for the following fixed element values:

$l = \frac{3}{4}$ wavelength at f_0',

$f_0' = 18$ Gc,

$f_0 = 1.5$ Gc,

$C_0 = 0.6$,

$a = 0.32$.

Choosing the stub to be resonant at the sideband frequency helps achieve the broadest bandwidth. For the same reason, the stub should be the shortest resonant length that allows reasonable values of d/b and C_A.

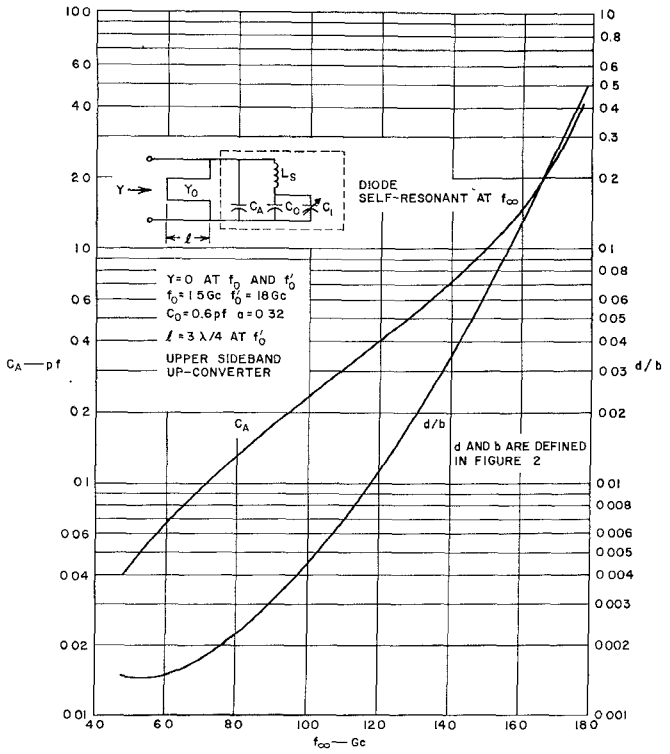

Fig. 3—Data for the design of the diode circuit of an upper-sideband up-converter.

III. The Up-Converter

The results of the preceding section were applied to upper-sideband up-converter design, following the method of Part X of Matthaei,[1] where a six-reactive element low-pass prototype filter was used in the design of an up-converter having three resonators at the signal frequency and three resonators at the upper-sideband frequency. Fig. 4 shows the basic circuit diagram of the up-converter. The diode circuitry of Fig. 2 is used. The series-resonator reactance X_2, resonant at signal frequency, is assumed to present a very high reactance at the upper-sideband frequency. Similarly, the series-resonator reactance X_2', resonant at the sideband frequency, is assumed to present a very high impedance at signal frequency.

To determine the resonator slope parameters b_1 and b_1' (see Matthaei[1]) it is necessary to use Fig. 2(d) where it is seen that the diode resonators consist of the stub, C_A and B_{11}^e or B_{22}^e. The slope parameters of the diode circuitry resonances are

$$b_1 = \pi f_0 \left\{ C_A + \frac{lY_0}{c} \csc^2 \frac{2\pi f_0 l}{c} + \frac{C_0^s}{a^2 - \gamma_0\gamma_0'} \left(\gamma_0' + \frac{2f_0 f_0'}{f_\infty^2} \right) + 2\left(\frac{f_0}{f_\infty}\right)^2 \frac{C_0^s \gamma_0'}{(a^2 - \gamma_0\gamma_0')^2} \left[\gamma_0' + \gamma_0 \frac{f_0'}{f_0} \right] \right\} \quad (4)$$

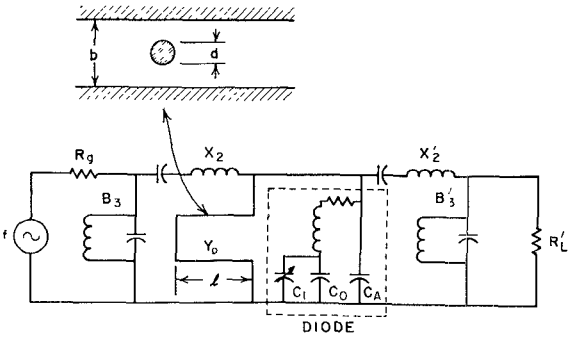

Fig. 4—Up-converter circuit diagram.

at the signal frequency, and

$$b_1' = \pi f_0' \left\{ C_A + \frac{lY_0}{c} \csc^2 \frac{2\pi f_0' l}{c} + \frac{C_0^s}{a^2 - \gamma_0\gamma_0'} \left(\gamma_0 + \frac{2f_0 f_0'}{f_\infty^2} \right) + 2\left(\frac{f_0'}{f_\infty}\right)^2 \frac{C_0^s \gamma_0}{(a^2 - \gamma_0\gamma_0')^2} \left[\gamma_0 + \gamma_0' \frac{f_0}{f_0'} \right] \right\} \quad (4)$$

at the upper-sideband frequency. The equation giving the fractional bandwidth of the up-converter is

$$w = \sqrt{\frac{(B_{12}^e B_{21}^e)_0}{b_1 b_1'} \frac{\Re_g}{\Re_L} \frac{f_0'}{f_0}} \left(\frac{\Omega_1 l_1}{r_L} \right), \quad (5)$$

where $\Re_g$, $\Re_L$, Ω_1, l_1, and r_L are parameters of the low-pass prototype filter as discussed in Matthaei.[1] The first fraction under the radical depends critically upon the diode resonant frequency ω_∞, as was mentioned in the discussion of the diode circuitry. Fig. 5 illustrates this bandwidth dependency for an up-converter designed using a six-reactive element, 0.5-db ripple, low-pass prototype filter (to give an amplifier with three input and three sideband output resonators), with the same diode and diode-circuitry values assumed for Fig. 3. A maximum fractional bandwidth is reached for roughly the $f_\infty = \omega_\infty/2\pi$ value predicted in Fig. 1. While this maximum is fairly broad, a poorly selected diode or poorly designed diode-circuit can seriously reduce the available bandwidth of an up-converter.

An electronic computer was programmed to calculate diode circuit element values and up-converter bandwidth from (3) and (5), and resonator slope parameters and terminations from the following equations, determined from Matthaei.[1]

$$R_g = \frac{\Omega_1 l_1}{w r_L b_1}, \quad x_2 = \frac{\Omega_1 c_2 r_L}{w} R_g, \quad b_3 = \frac{\Omega_1 l_3}{w r_L R_g},$$
$$R_L' = \frac{\Omega_1 l_1}{w' r_L b_1'}, \quad x_2' = \frac{\Omega_1 c_2 r_L}{w'} R_L', \quad b_3' = \frac{\Omega_1 l_3}{r_L w' R_L'}. \quad (6)$$

Fig. 6 is the two-frequency circuit diagram used in connection with (6) to determine gain as a function of

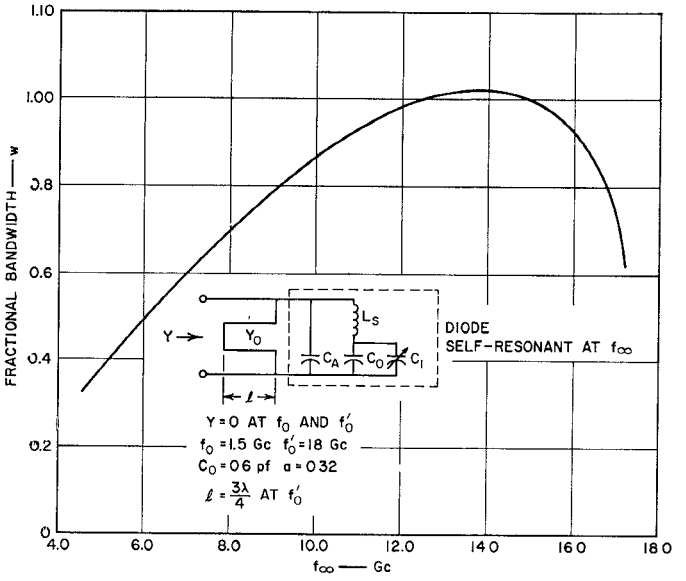

Fig. 5—Approximate fractional bandwidth for case of upper-sideband up-converter with three input and three sideband-output resonators designed from a prototype with 0.5-db Chebyshev ripple.

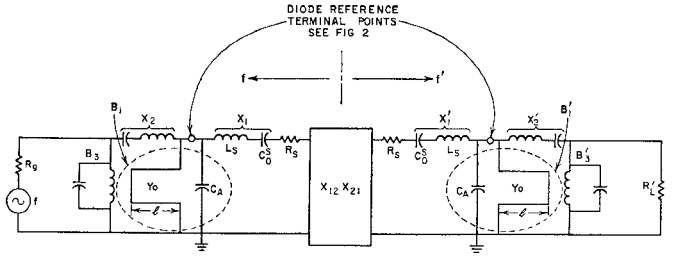

Fig. 6—Two-frequency equivalent circuit for upper-sideband up-converter.

frequency, following the method of Matthaei.[1] Equations for gain were also programmed for an electronic computer.

A diode was assumed having properties similar to those of Micro State Electronics Corporation gallium arsenide varactor MS 2504. An input center frequency of 1.50 Gc and an output center frequency of 18.0 Gc were chosen. The diode resonant frequency was calculated to be 12.52 Gc, which is very close to the approximate optimum of seven-tenths of the upper sideband frequency, as discussed in the preceding section. The following are the assumed and calculated circuit and parameter values for an up-converter using this diode:

$C_0 = 0.60$ pf
$a = 0.32$
$L_s = 0.30$ nh
$R_{s_s} = 2.46\ \Omega$
$C_{0_s} = 0.5386$ pf
$C_1 = 1.683$ pf
$f_0 = 1.50$ Gc
$f_0' = 18.0$ Gc
$f_\infty = 12.52$ Gc
$C_A = 0.460$ pf
$Y_0 = 3.742$ mmho
$l = 0.492$ in ($\frac{3}{4}$ wavelength at f_0')
$d/b = 0.0148$
$R_g = 270\ \Omega$
$R_L' = 309\ \Omega$
$w = 1.00$ (fractional bandwidth for $R_s = 0$, and lumped elements).

The circuit elements were determined on the assumption that the diode series resistance was zero. Then, transducer gain was computed as a function of frequency, both with and without series resistance included. These gain curves are shown on Fig. 7. The curve labelled "ideal" is the power gain (rather than transducer gain) required by the Manley-Rowe relations, $10 \log_{10} f'/f$ where f' is the upper-sideband frequency and f the signal frequency. No upper-sideband up-converter can have a transducer gain greater than this for given signal and upper-sideband frequencies. The peaks of the curve for no diode resistance ($R_s = 0$) depart from the curve labelled "ideal" at the higher frequency end of the band, because the stub no longer approximates a lumped inductance, as was assumed at band center. The loss in gain with diode resistance, indicated by the curve labelled "actual," is due almost entirely to currents at the upper-sideband frequency. Referring to Fig. 6, the termination, R'_L is less than R_s. This loss cannot be avoided in this case. However, the "actual" curve is probably very close to the performance that could be realized in practice. The 3-db bandwidth of this curve is 77 per cent, which is well over an octave.

This up-converter was found to have a noise figure of 0.47 db at the band-center of 1.5 Gc, where noise figure F is based on the definition

$$F = 10 \log_{10} \cdot \left(\frac{\text{Detected Noise Power of Actual Amplifier}}{\text{Detected Noise Power of Ideal Amplifier}} \right) \text{db}.$$

The low noise figure is achieved in spite of the loss of gain caused by the diode resistance, because this loss of gain occurs after the signal has been amplified.

To illustrate the possibility of using other diodes, a diode similar to Microwave Associates MA-4252 was assumed. This diode has a smaller shunt capacitance and a larger series inductance than the Micro State MS-2504, but otherwise is assumed to be electrically the same. Shunt capacitance C_A was taken as 0.2 pf, which required that f_∞ be about 9.5 Gc according to Fig. 3. This means that the diode inductance must be 0.52 nh, which is lower than the manufacturers specified value of 0.8 nh, but measurements made at SRI have indicated that considerably lower values of L_s are found on actual diodes if the diode is properly mounted. The fractional bandwidth graph Fig. 5 then gave a value

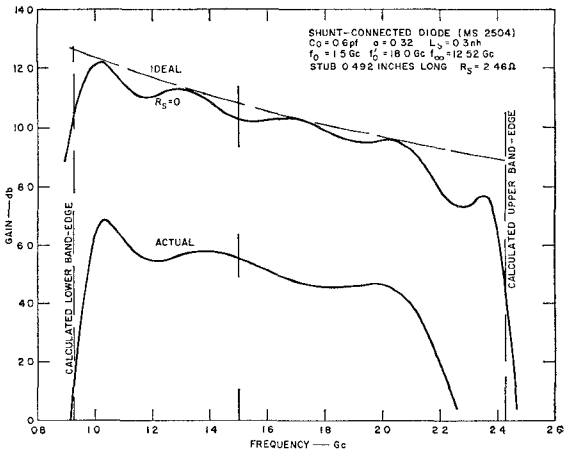

Fig. 7—Gain of upper-sideband up-converter with three input and three sideband-output resonators designed from a prototype with 0.5-db Chebyshev ripple.

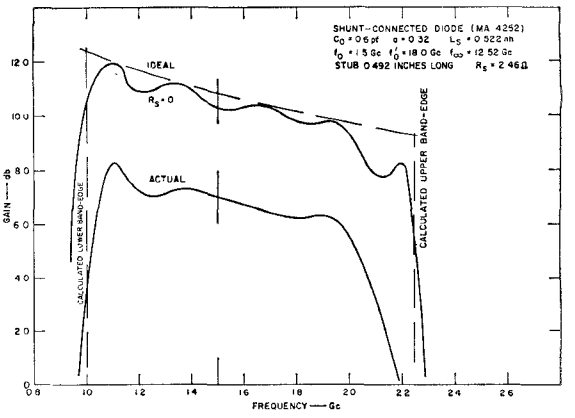

Fig. 8—Gain of upper-sideband up-converter with three input and three sideband-output resonators designed from a prototype with 0.5-db Chebyshev ripple.

for w of 0.83. The gain vs frequency curve for the up-converter using this diode is shown in Fig. 8. Its 3-db bandwidth, allowing diode losses, is about 69 per cent, which is smaller than that of the other up-converter, but it has greater gain and a noise factor of only 0.37 db or 0.1 db less than the wider-band up-converter.

The up-converter performance curves for $R_s = 0$ indicate the validity of the design technique and show the limit of performance that might be achieved with less lossy diodes. The "actual" curves indicate performance that it should be possible to approach using presently available diodes. Fig. 9 is a picture showing how a wideband up-converter of this sort might be constructed

The entire structure shown in plan in Fig. 9 lies between parallel ground planes. The input filter is in thick-bar stripline construction.[5] Although Fig. 9 shows semilumped inductance and capacitance for each resonator, simple quarter-wavelength-long shorted stubs would work also, as indicated in Fig. 14(a) of Matthaei.[5] In any case, it would be desirable to use the design technique of Matthaei[5] to accurately achieve the broad bandwidth required for the input filter.

The low-pass filter[6] between the diode and Resonator 2 of the input filter presents a very large reactance at the diode to the pump and upper-sideband signals, which are well within the stop-band of the filter. Thus, it isolates these signals from the input circuitry. But, at the input frequency, the low-pass filter acts as a quarter-wavelength section of line, because this frequency is well within the passband of the low-pass filter.

The diode and resonating stub are constructed as shown in Fig. 2. The diode stub is used to couple in-

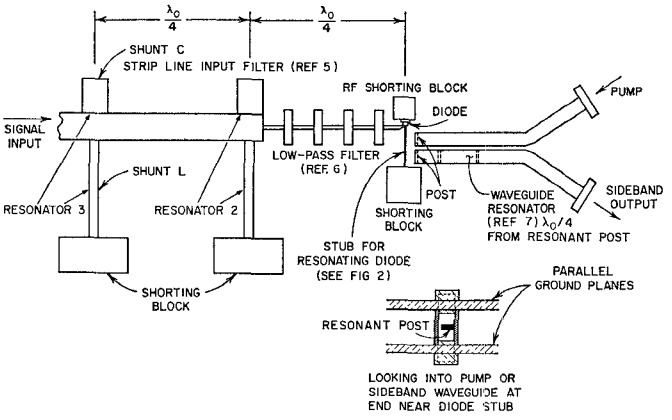

Fig. 9—Possible form for fabricating up-converter.

ductively to resonant posts in both the pump and upper-sideband waveguide filters.[7] A detail of one of the waveguide coupling structures is shown at the bottom of Fig. 9. The dimensions of the coupling structure and the best distance from the resonant post in the waveguide to the diode stub would be found experimentally, although other dimensions of the waveguide filters could be found by the methods of Cohn.[8]

IV. The Nondegenerate Parametric Amplifier

Nondegenerate parametric amplifiers using the diode circuitry described in the previous sections were designed following the general principles of Matthaei.[1] However, some of the equations given in Matthaei[1] no longer hold because of the type of diode circuitry to be assumed in the present analysis.

[5] G. L. Matthaei, "Design of wide-band (and narrow-band) band-pass microwave filters on the insertion loss basis," IRE Trans. on Microwave Theory and Techniques, vol. MTT-8, pp. 580–593; November, 1960.

[6] S. B. Cohn, "Very High Frequency Techniques," McGraw-Hill Book Company, Inc., New York, N. Y., vol. II, chs. 26 and 27; 1947.

[7] The use of inductive coupling between the diode stub and resonant posts in waveguide structures is, of course, only one of numerous possible ways of coupling the sideband and pump circuits to the diode circuit. In the example in Fig. 9 three resonators operating at the sideband frequency are formed by the resonance of the diode circuit at f_0', the resonance of a resonant post (the post may be regarded as part of a resonant iris), and a half-wavelength resonator having inductive irises at each end.

[8] S. B. Cohn, "Direct-coupled-resonator filters," Proc. IRE, vol. 45, pp. 187–196; February, 1957.

A physical circuit diagram is given in Fig. 10. Circuit simplification is achieved by letting the diode resistance act as the idler (lower sideband) termination. An ideal, lossless circulator is assumed. The design method will be explained with the aid of the two-frequency circuit diagram shown in Fig. 11. At band center the resonator reactance $X_2=0$ at the signal frequency. At the idler frequency X_2 is very large, so only the circuit shown to the right of the box labelled $X_{12}X_{21}$ plays any significant role for that frequency. At band center, the diode circuitry is resonated so that $Z_b'=0$, leaving R_s only to act as the idler load. The idler frequency is selected to be the highest resonant frequency that can be achieved with the circuit to the right of $X_{12}X_{21}$. This occurs when the diode-resonating stub is an odd number of quarter wavelengths long, and thus appears as an open circuit across C_A. With this constraint, the idler center frequency is

$$f_0' = \frac{1}{2\pi\sqrt{\dfrac{L_d C_0^s C_A}{C_0^s + C_A}}}. \tag{7}$$

Now since[1]

$$Z_2 = \frac{-X_{12}X_{21}}{(Z_a')^*}, \tag{8a}$$

for $f'=f_0'$

$$Z_2\Big|_{f'=f_0'} = \frac{-X_{12}X_{21}}{R_s}, \tag{8b}$$

where Z_2 and Z_a' are defined in Fig. 11, $(Z_a')^*$ is the complex conjugate of Z_a', and $X_{12}X_{21}$ is purely real and is defined in Matthaei.[1] Then C_A is selected to be the smallest value of capacitance that can be reliably obtained in practice, because this selection helps keep f_0' high, and also leads to the largest bandwidth.

Next, the stub admittance is adjusted so that the imaginary part of Z_3 in Fig. 11 is zero. This resonates the diode circuitry at the signal frequency. The number of odd quarter-wavelengths of the stub at the idler frequency is again selected to be the smallest that gives reasonable values of d/b.

Then R_g, the termination to be presented by the circulator, is calculated to give the desired band-center gain G_{T0} in decibels.

Formulas expressing the results of this procedure are as follows:

$$Y_0 = \left[2\pi f_0 C_A + \frac{R_s}{2\pi f_\infty C_0^s A}\left(\frac{f_\infty}{f_0} - \frac{f_0}{f_\infty}\right)\right]\tan\frac{2\pi f_0 l}{c}$$

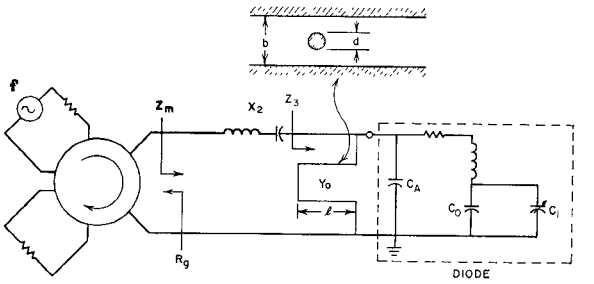

Fig. 10—Circuit diagram for a nondegenerate parametric amplifier which uses the diode resistance for the idler termination.

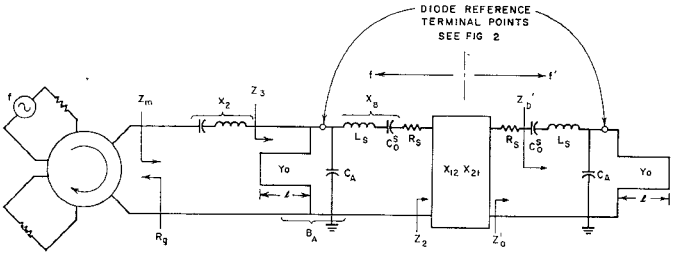

Fig. 11—Two-frequency equivalent circuit for the nondegenerate parametric amplifier in Fig. 10.

$$R_g = \left[\frac{A}{R_s^2 - \left(\dfrac{a}{2\pi C_0^s}\right)^2 \Big/ f_0 f_0'}\right]\left(\frac{1 - 10^{G_{T0}/20}}{1 + 10^{G_{T0}/20}}\right) \tag{9}$$

where

$$A = \frac{\left[R_s^2 - \left(\dfrac{a}{2\pi C_0^s}\right)^2 \Big/ f_0 f_0'\right]^2 + \left(\dfrac{R_s}{2\pi C_0^s f_\infty}\right)^2\left(\dfrac{f_0}{f_\infty} - \dfrac{f_\infty}{f_0}\right)^2}{R_s}$$

and

$$f_\infty = \frac{1}{2\pi\sqrt{L_d C_0^s}}. \tag{10}$$

A difficulty arises in attempting further synthesis of an optimum input filter, because Z_2 in Fig. 11 appears to be, approximately, a negative resistance shunted by a resonator composed of *negative* inductance and *negative* capacitance. These negative elements must be transformed through the diode-circuitry branches X_B and B_A before a physically available set of terminals is reached (at Z_s).

From the filter synthesis point of view, a low-pass prototype is needed in which the first reactive element is negative and the next is positive. As far as is known, theory for the design of such a prototype does not exist at this time. Therefore, the following empirical approach was taken to broad-banding the parametric amplifier.

First, a simple amplifier is designed using the diode circuitry values given by the above equations (7)–(10). This amplifier would appear like that shown in Fig. 10, but with X_2 omitted. Then, gain and input impedance (Z_3) are programmed on an electronic computer. Some

increase in bandwidth at the expense of gain is now possible simply by changing the pump frequency. This displaces the idler frequency with respect to the design value of the diode-circuitry resonance. The resulting effect is as though the idler frequency were constant and the diode-circuitry resonance were changed instead. Although two tuned circuits are involved (*i.e.*, the signal and the idler tuned circuits), only single-peaked responses were obtained in the calculations—which is to be expected since as a result of (8a) the idler tuned circuit reflects through $X_{12}X_{21}$ so as to look much like a circuit with $-L$ and $-C$ in parallel. (The reactance slope of this reflected reactance then simply adds to that of the input resonator instead of subtracting as occurs in coupled-resonator filters.) The following table gives some examples of bandwidth obtained for various pump frequencies for a 1.5-Gc amplifier to be described more fully later. These computed data are for the case of a single input resonator and a single idler resonator (each formed by a resonance of the diode circuit) with all design parameters held constant except for the pump frequency. (This is the case of Figs. 10 and 11 with resonator X_2 removed and some other means provided for preventing leakage of the idler signal.)

Pump Frequency, Gc	3-db Bandwidth	Maximum Gain
19.545 (Design value)	9%	16 db
19.595	12%	14.5 db
19.695	15.5%	12 db

In general, it is advisable to add a resonator, such as X_2 in Fig. 10, not only to broaden the bandwidth but also to keep the idler frequency off the input line. It was assumed in determining the diode-circuitry design equations that the idler frequency was isolated from the input line by an apparent open circuit seen at the diode terminals at idler frequencies. This open circuit is simulated by the reactance of X_2 at the idler frequency.

The following procedure is used to find suitable values for the resonator slope parameter x_2 and resonant frequency f_2 of the resonator X_2. The input impedance, Z_3 for the amplifier without X_2, is plotted as a function of frequency. An example of such a plot is shown in Fig. 12. The imaginary part of Z_3, the negative of the real part of Z_3, and the terminating resistance R_g are plotted together on the center graph. The gain G_T is given by

$$G_T = 10 \log_{10} |\Gamma|^2, \tag{11}$$

where

$$|\Gamma|^2 = \left| \frac{Z_m - R_g}{Z_m + R_g} \right|^2,$$

and Z_m is as defined in Fig. 10. Before X_2 is added, Z_m is the same as Z_3, as can be seen on Fig. 10. At the frequency where the imaginary part of Z_m is zero,

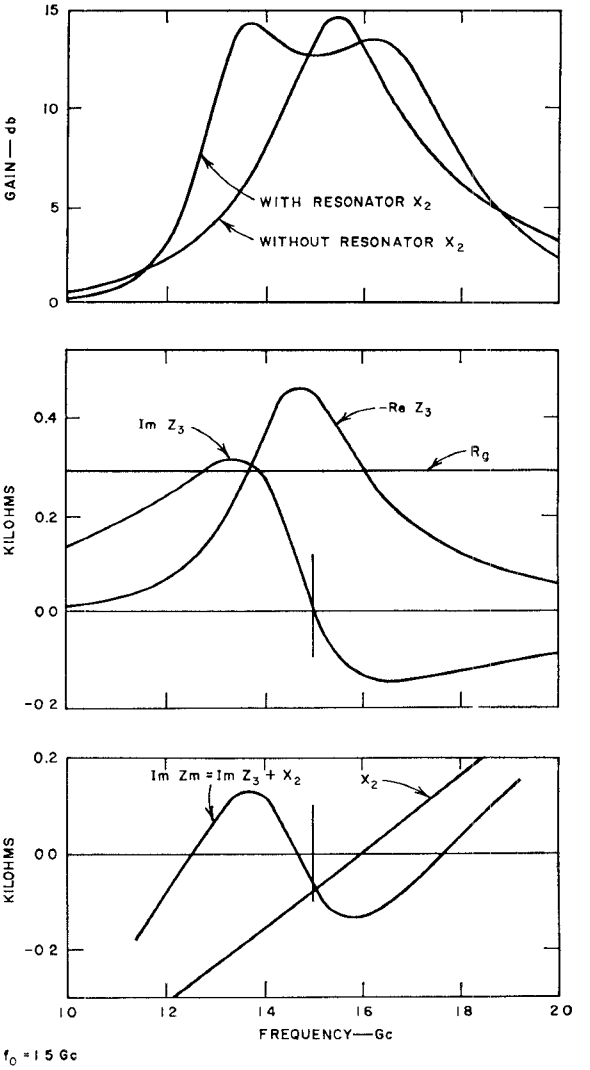

Fig. 12—Gain and impedances computed in broad-banding the amplifier in Figs. 10 and 11.

$$|\Gamma|^2 = \left| \frac{\text{Re } Z_3 - R_g}{\text{Re } Z_3 + R_g} \right|^2. \tag{12}$$

Notice that Re Z_3 is negative.

At the two frequencies where R_g+Re Z_3 is zero (where $-$Re Z_3 and R_g cross on the center graph of Fig. 12),

$$|\Gamma|^2 = \left| \frac{2R_g}{\text{Im } Z_m} \right|^2. \tag{13}$$

These two frequencies are denoted as the critical points, because, were the input reactance zero there, the amplifier would oscillate. Observe that the peaks in the gain curve (with resonator X_2) of Fig. 12 occur at very nearly the same frequencies as the critical points, and that the dip in the gain curve occurs at the frequency where $-$Re Z_3 is a maximum (provided X_2 has

been adjusted to allow only a small value of Im Z_m at that frequency).

Therefore, one point of reactance X_2 is located equal to and opposite Im Z_3 at the frequency where $-\text{Re}\ Z_3$ is maximum. This gives the greatest band-center gain, which can be calculated from (11) and (12). Then, X_2 is approximated by a straight line passing through this point, and having a slope such that Im $Z_m = \text{Im}\ Z_3 + X_2$ has approximately the same absolute value at the two critical points. An example of X_2 and the total reactance are shown in the lower graph of Fig. 12. The gain at the peaks can then be calculated by (11) and (13). Peak gains are much more sensitive to X_2 than is the gain at the dip, and so the center frequency and slope parameter of X_2 may be readjusted to modify the peaks without affecting the gain at the dip greatly. The foregoing procedure is most easily carried out by plotting the negative of X_2 on the same graph with Im Z_3. Then the difference between the two curves is the value of Im Z_m, at a given frequency.

The slope parameter[1] x_2 for resonator X_2 is found from

$$x_2 = \frac{f_2}{2}\frac{\Delta X_2}{\Delta f} \tag{14}$$

where $\Delta X_2/\Delta f$ is the slope of the line X_2 on the graph.

Finally, the gain near the dip can be increased or decreased by increasing or decreasing the value of the terminating resistance R_g. Flattening the gain curve in this manner decreases the total bandwidth, but this is compensated for by greater gain.

Fig. 13 shows the results of this procedure for a parametric amplifier using the micro-state diode assumed previously. The following assumed and calculated values apply.

$C_0 = 0.6$ pf $\quad C_A = 0.5$ pf

$a = 0.32$ $\quad l = 0.49$ in

$L_s = 0.3$ nh $\quad d/b = 0.0095$

$R_s = 2.46\ \Omega$ $\quad R_g = 292\ \Omega$.

$f_0 = 1.5$ Gc

$f_0' = 18.045$ Gc

$f_\infty = 12.52$ Gc

The values for the pump frequency f_p, the center frequency f_2 of resonator X_2, and the slope parameter x_2 of resonator X_2 are given for each curve on Fig. 13.

The bell shaped curve is the amplifier response without using resonator X_2, and the other curves show the bandwidth improvement obtained for various pump frequencies and different adjustments of resonator X_2. In this case the termination R_g was not changed from its design value found by (9).

Using the same diode, another parametric amplifier was designed to operate in C band. The same idler frequency was used as for the lower frequency amplifier because the idler frequency is determined by the diode element values, in accordance with (7). The stub length was one-quarter wavelength (0.163″) at the idler frequency and d/b was found to be 0.55. In this case the pump frequency was kept at its design value of 24.045 Gc, a slope parameter $x_2 = 261$ ohms and a center frequency of 6.35 Gc were used for resonator X_2. Then, the value of the termination R_g was adjusted to modify the shape of the response curve. Fig. 14 gives the gain vs frequency for $R_g = 60$ ohms and $R_g = 70$ ohms. This illustrates how the pass band can be flattened by raising the terminating resistance. Before using resonator X_2 and adjusting the termination, the amplifier had a bandwidth of only about 140 Mc. After broad-banding, the bandwidth was 900 Mc for the 70-ohm termination and 1070 Mc for the 60-ohm termination.

Noise factor at band center was calculated for these amplifiers also, and found to be 0.40 db for the amplifier operating at 1.5 Gc, and 1.57 db for the amplifier operating at 6 Gc. These parametric amplifiers might be constructed much like the up-converter of Fig. 9, but with Resonator 3 and the sideband output waveguide structure removed.

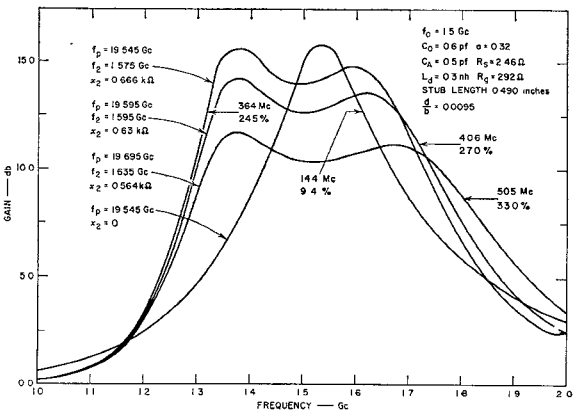

Fig. 13—Gain of an L-band amplifier of the form in Fig. 10, for various circuit conditions.

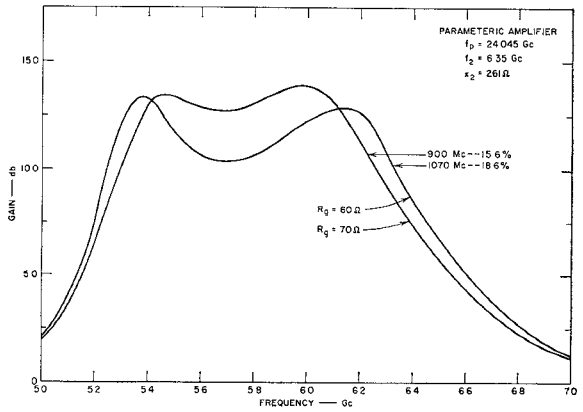

Fig. 14—C-band nondegenerate parametric amplifier gain for different values of terminating resistance.

VI. Further Comments and Conclusions

Matthaei[1] previously discussed the importance of minimizing the number of resonances in the diode circuit in order to obtain an up-converter or parametric amplifier design having maximum bandwidth. The results summarized in Fig. 1 of this paper are for the case where there is only one resonance between the signal- and sideband-frequency resonances. This study showed that even with only one resonance between the signal and sideband resonances, there will be a wide range in the bandwidth capability of the resulting amplifier design depending on the frequency at which the additional resonance of the diode circuit occurs. Fig. 5 of this paper illustrated this fact for the case of an upper-sideband up-converter using a diode resonated in shunt. From Fig. 5 it is seen that having a suitable diode series-resonant frequency f_∞ is very important in obtaining a design with maximum or nearly maximum bandwidth. Actually, for the case of Fig. 5 there are other resonances besides f_∞ between frequencies f_0 and f_0', because the resonating stub was chosen to be three-quarters of a wavelength long at f_0'. However, the deleterious effects of these extra resonances[9] are minimized in this case because with the stub three-quarter-wavelengths long at f_0', the stub presents a very high impedance in the sideband frequency range so that the stub has relatively little effect on the susceptance characteristic in that band. Meanwhile, at the signal frequency band the electrical length of the stub is sufficiently short so that the stub operates much like a lumped impedance.

The analysis of the effects of the diode resonances was made in terms of upper-sideband up-converters, but it appears probable that the results regarding the optimum frequency for a resonance between the signal- and sideband-frequency resonances would also provide a useful guide in the design of other types of wideband parametric devices such as lower-sideband up-converters and nondegenerate parametric amplifiers.

Using a diode-resonating circuit such as that in Fig. 2(a), provision for tuning the circuit so as to accommodate a range of diode parameters can be made by providing capacitive tuning screws near the diode so as to vary the effective diode package capacitance C_A [see Fig. 2(b)]. This adjustment would be used to tune the diode to resonance at f_0'. Tuning the diode to resonance at f_0 could then be accomplished by tuning screws which introduce capacitance shunting the stub at a point a distance away from the diode. The location of these tuning screws should be chosen so they are at a voltage null point on the stub at frequency f_0' (assuming stub is over $\lambda_0'/4$ long at f_0'). In this way, this second set of screws would be useful for tuning the circuit to the input midband frequency f_0, but would have no effect at the sideband (or idler) frequency f_0'. It may be desirable in some cases to also provide for altering the impedance level reflected to the diode by the broadbanding filter structures at the input and possibly also at the sideband (if a broadbanding structure is used for the sideband frequencies), in order to correct for variations in the C_1 coefficient[1] of different diodes. This can be accomplished by use of filter structures with adjustable couplings. In the case of Fig. 9, the coupling to the sideband filter structure can be altered by sliding the lower waveguide structure back and forth. To obtain adjustable impedance levels in input filter structures, the use of interdigital filter[10] or comb-line filter[11] structures with adjustable spacing between two or more of the resonator elements may prove practical.

The procedure outlined in Section IV of this paper provides a systematic means for designing wide-band, nondegenerate parametric amplifiers which use the diode parasitic resistance as the idler termination. This procedure does require computation of the Z_3 impedance characteristic (shown at the center of Fig. 12) for the diode and frequency parameters to be used. This is tedious to do by hand. But since computer service is now so widely available, the need to compute and plot the Z_3 characteristic of the diode-resonator circuit should not be a drawback for most designers. The comments made above regarding means for making tuning adjustments on the diode circuit and means for adjusting the impedance level of the signal input circuit also apply for the case of nondegenerate parametric amplifiers.

In this paper, it has been assumed that the pump circuit is loosely coupled to the diode circuit, so that the pump circuit will not introduce any additional resonances of sufficient bandwidth to noticeably affect the diode-circuit performance at the signal and sideband frequencies.

[9] Because of narrow-band-type approximations used in computing the curve in Fig. 5, that curve does not entirely account for the bandwidth-reducing effects of these extra diode resonances. However, the computed responses in Fig. 7 do fully account for all such effects.

[10] G. L. Matthaei, "Interdigital band-pass filters," IRE Trans. on Microwave Theory and Techniques, vol. 10, pp. 479–491; November, 1962.

[11] G. L. Matthaei, "Comb-line band-pass filters of narrow or moderate bandwidth," *Microwave J.*, vol. VI, pp. 82–91; August, 1963.